Uluslararası İleri Doğa Bilimleri ve Mühendislik Araştırmaları Dergisi
Sayı 8, S. 63-73, 7, 2024

Araştırma Makalesi

IJANSER

International Journal of Advanced Natural Sciences and Engineering Researches
Volume 8, pp. 63-73, 7, 2024

Research Article

https://as-proceeding.com/index.php/ijanser
ISSN: 2980-0811

Robot Arm Manipulator Position Control Using Fractional Order PID Enhanced by Hybrid PSOGSA

Mohammed Yousri Silaa[1, 3*], Aissa Bencherif [1], Ilyas Rougab[2] and Oscar Barambones[3]

[1]Telecommunications Signals and Systems Laboratory (TSS) University Amar Telidji, Laghouat, 03000 Algeria
[2]LACOSERE Laboratory, University Amar Telidji, Laghouat, 03000 Algeria
[3]Engineering School of Vitoria, University of the Basque Country UPV/EHU, Vitoria, 1006 Spain
[*](moh.silaa@lagh-univ.dz) Email of the corresponding author

(Received: 07 August 2024, Accepted: 28 August 2024)

(5th International Conference on Engineering and Applied Natural Sciences ICEANS 2024, August 25-26, 2024)

ATIF/REFERENCE: Silaa, M. Y., Bencherif, A., Rougab, I. & Barambones, O. (2024). Robot Arm Manipulator Position Control Using Fractional Order PID Enhanced by Hybrid PSOGSA. *International Journal of Advanced Natural Sciences and Engineering Researches*, 8(7), 63-73.

Abstract – This paper introduces a control strategy using the fractional order proportional integral derivative (FOPID) controller, for regulating a 2-DOF robot manipulator position. While widely used in the industry domain, the conventional proportional integral derivative (PID) controller exhibits limitations in handling external disturbances, making it less robust. The FOPID controllers offer improved robustness, particularly against uncertainties and external disturbances. In this study, a hybrid swarm optimization and gravitational search algorithm (PSOGSA) is employed in order to tune and optimize the controller gains. The efficacy of the proposed control approach is systematically compared with the conventional PID controller. Numerical simulations demonstrate the superior performance of the proposed FOPID methodology over the traditional PID controller, showcasing quantifiable improvements in root mean squared error (RMSE), FOPID achieves RMSE values of 0.084813, and 0.044337 in the position's trajectories. These results illustrate the exceptional performance of the FOPID enhanced by PSOGSA in achieving precise control. The proposed FOPID presents advantages in accurate tracking trajectory, adaptability under noises and computational efficiency. This study contributes to the progress of robust control techniques for 2-DOF, highlighting the potential of FOPID to improve trajectory tracking in practical, real-world applications.

Keywords – Robot Manipulator; FOPID; PID; PSOGSA; Trajectory Tracking.

I. INTRODUCTION

Robot manipulators play an important role in industrial domains and enhancing their performance requires effective control methods [1]. Various control approaches have been extensively explored and implemented in the literature to achieve precise, robust and efficient control systems [2–6]. These techniques play a vital role in enhancing the performance and capabilities of robot manipulators. For instance, Jin et al. [7] introduced a practical nonsingular terminal sliding mode control for robot manipulators, incorporating time-delay estimation to ensure fast convergence. This method requires no prior knowledge of robot dynamics. Bi [8] designed a symmetrical fuzzy PID algorithm for optimized control of a two-degree-of-freedom (2-DoF) manipulator. The algorithm adjusts P, I and the D values based

on error rate principles. The mathematical model establishes a functional relationship between input driving force and output rotation angle vectors. Trajectory planning algorithms, employing gradient model control, effectively calculate end-effector trajectories. Experimental results confirm the algorithm's efficacy, showcasing its potential for real-world applications. Jouila et al. [9] introduced a robust adaptive control method for a two-link robot manipulator using a Non-Singular Fast Time Sliding Mode (NFTSM) controller with a Wavelet Neural Network (WNN). The WNN approximates uncertainties and a compensation term minimizes their impact. Online adaptive learning tunes controller parameters, ensuring high tracking accuracy and reducing chattering. Simulations on a two-link robotic arm demonstrate superior performance compared to other advanced control strategies. Efe [10] proposed an innovative parameter adjustment approach using an adaptive neuro-fuzzy inference system to enhance the robustness of fuzzy sliding mode control. The method, employing fractional order integration in parameter tuning, demonstrated improved tracking performance, robustness and insensitivity to external disturbances. Kumar et al. [11] applied a genetic algorithm (GA) optimization method to interval type 2 fuzzy PD plus integral controllers for redundant robot manipulators, demonstrating improved trajectory tracking and robustness. Ouyang et al. [12] proposed a novel PD with sliding mode control approach for trajectory tracking in multi-degree-of-freedom linear translational robotic systems, leveraging the simplicity of PD control and the robustness of sliding mode control to model uncertainty. In addition to these specifics methods, various control systems have been explored to enhance trajectory tracking in robot manipulators [13–19]. The ant colony optimization (ACO) algorithm was initially introduced by Mirjalali et al. [20], marking significant progress in problem optimization [21]. Serving as a meta-heuristic optimization system, ACP mimics the foraging behavior of ant colonies to tackle diverse problem-solving tasks. Its applications span various domains, including minimizing power losses in power distribution networks [23], optimizing fitness functions for fuzzy systems in image segmentation [24] and determining optimal parameters for degradation trajectories through a weighted fusion function [25]. In the field of robotics, an optimized PID control for a quadruped robot is proposed, leveraging ACO to fine-tune the PID controller parameters for achieving the desired trajectory. Comparative analysis against other optimization algorithms, such as GA and PSO, reveals ACO's superior performance [26]. This paper proposes a control approach utilizing fractional-order proportional- integral-derivative (FOPID) in order to improve the 2-DOF tracking position performance. Subsequently, a hybrid PSOGSA is employed to fine-tune the FOPID controller parameters. Furthermore, the performance of the proposed control method is compared with the PID, into its effectiveness. The remaining sections of this paper are organized as follows: Section 2 provides a detailed description of the dynamic modeling of a 2-DOF robotic manipulator. The principles and the implementation of FOPID is discussed in Section 3, while Section 4 covers the details of PSOGSA. Section 5 presents the simulation results and the paper concludes by summarizing the findings and contributions in the final section.

II. DYNAMIC MODELING OF A 2-DOF ROBOT MANIPULATOR

Dynamic modeling of a 2-DOF robot manipulator is a crucial process in robotics that involves deriving equations to describe the motion and behavior of a two-jointed robotic system as shown in Fig 1. The dynamic modeling of the 2-DOF arm robot manipulator can be expressed according to the equation as follows [27]:

$$B(q)\ddot{q} + C(q,\dot{q})\dot{q} + G(q) = \tau \qquad (1)$$

Where, $q,\ \dot{q},\ \ddot{q} \in R^2$ are the vector of joint angles, the vector of joint velocities and the vector of joint accelerations respectively. B(q) $\in R^{2\times2}$ is the inertia matrix, $C(q,\ \dot{q}) \in R^2$ is the Coriolis and centrifugal matrix, $G(q) \in R^2$ is the gravitational vector and $\tau \in R^2$ is the vector of joint torques. *B(q), C (q, $\dot{q}$)* and *G(q)* are given in Appendix A. Therefore, the previous equation can be written as follows [27]:

$$\ddot{q} = -B^{-1}C(q,\dot{q})\dot{q} - B^{-1}G(q) + B^{-1}(q)\tau \qquad (2)$$

The dynamic equation governing the motion of a 2-degree-of-freedom robot manipulator is given as follows:

$$\ddot{q} = -M\dot{q} - NG(q) + Ou(t) \quad (3)$$

Where, $M = B^{-1} C (q, \dot{q}) N = B^{-1} (q)$, $O = B^{-1} (q)$ and $u(t) = \tau$ represents the control vector. Parameter uncertainties were introduced to account for variations in the system parameters hence, the previous equation can be defined as follows:

$$\ddot{q} = -(M + \delta M)\dot{q} - (N + \delta N)G(q) + (O + \delta O)u(t) \quad (4)$$

Where $\delta M, \delta N$ *and* δO represent uncertainties in parameter variations. The equation (5) can be written as follows [27]:

$$\ddot{q} = -M\dot{q} - NG(q) + Ou(t) + d(t) \quad (5)$$

Where, $d(t) = -\delta M\dot{q} - \delta N\, G(q) + \delta O u(t)$.

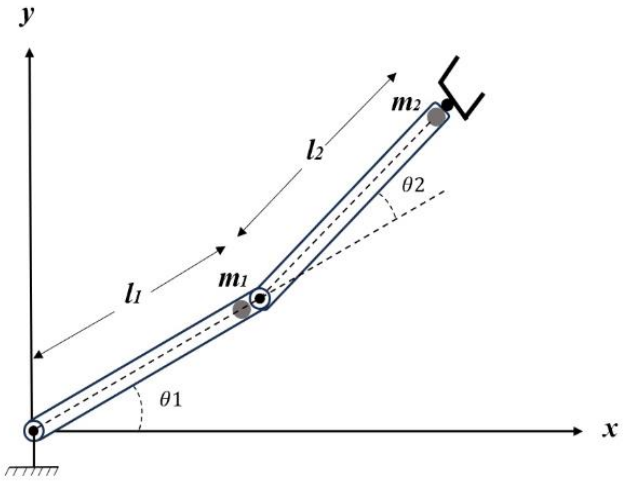

Fig. 1 Structure of a 2 DOF robot manipulator.

III. FRACTIONAL-ORDER PID CONTROLLER

A fractional-order PID (PFOPID) controller extends the traditional PID controller by introducing fractional calculus concepts. The FOPID controller includes fractional order integrators and differentiators, allowing for more flexibility and adaptability in controlling systems with non-integer order dynamics [28]. The FOPID controller equation can be expressed in a generalized form as follows [29]:

$$u(t) = K_p e(t) + K_i \int_0^t e(\tau) d^{\alpha}\tau + K_d \frac{d^{\beta} e(t)}{dt^{\beta}} \quad (6)$$

Where, *u(t)* is the control output, e(t) is the error signal, K_p is the proportional gain, K_i is the integral gain and K_d is the derivative gain. The terms $\int_0^t e(\tau) d^{\alpha}\tau$ and $\frac{d^{\beta} e(t)}{dt^{\beta}}$ represent the fractional-order integral and derivative, respectively. The fractional orders α and β can take any real values ∈ [0, 1] as shown in Fig 2.

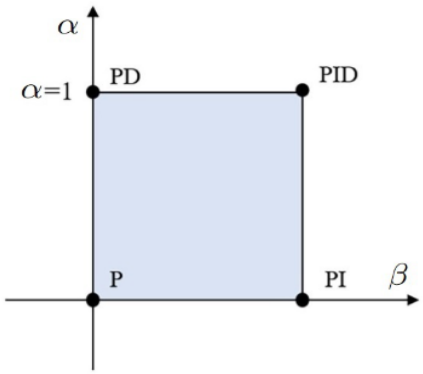

Fig. 2 Types of controllers according to α and β

IV. HYBRID PARTICLE SWARM OPTIMIZATION AND GRAVITATIONAL SEARCH ALGORITHM

The hybrid particle swarm optimization and gravitational search algorithm (PSOGSA) merges the exploration capabilities of particle swarm optimization (PSO) with the exploitation strengths of the gravitational search algorithm (GSA). In this hybrid algorithm, the velocity and position updates of particles are influenced by both PSO and GSA components. The velocity update equation combines the PSO components, where the cognitive term $c_1 r_1(p_{best} - x_i)$ and the social term $c_2 r_2(g_{best} - x_i)$ are added to the GSA component, the acceleration a_i derived from the gravitational forces. Mathematically, the velocity update for particle *i* at iteration *t* is given by [30]:

$$v_i(t+1) = \omega\, v_i(t) c_1 r_1 \left(p_{best} - x_i(t)\right) + c_2 r_2 \left(g_{best} - x_i(t)\right) + a_i(t) \quad (7)$$

Where, ω is the inertia weight, c_1 and c_2 are acceleration coefficients, r_1 and r_2 are random numbers in the range [0, 1], p_{best} is the personal best position, and g_{best} is the global best position. The acceleration a_i is calculated from the forces exerted by other particles based on the gravitational law which given as follows:

$$F_{ij} = G(t) = \frac{m_i(t) m_j(t)}{R_{ij}(t) + \varepsilon} \left(x_j(t) - x_i(t)\right) \quad (8)$$

Where, *G(t)* is the gravitational constant *which* calculated as follows:

$$G(t) = G_0 \times \exp\left(-\gamma \times iter/Maxiter\right)$$

Where, G_0 and γ are descending coefficient and initial value respectively. In addition, m_i and m_j are the masses of particles *i* and *j*, $R_{ij}(t)$ is the Euclidean distance between particles *i* and *j*, and ε is a small constant to avoid division by zero. The position update is then given as follows [30]:

$$x_i(t+1) = x_i(t) + v_i(t+1) \quad (9)$$

This hybrid approach leverages the local search capability of GSA to refine the search around promising regions identified by the global search ability of PSO, thus improving the overall optimization performance. The PSOGSA steps are presented in Figure 3.

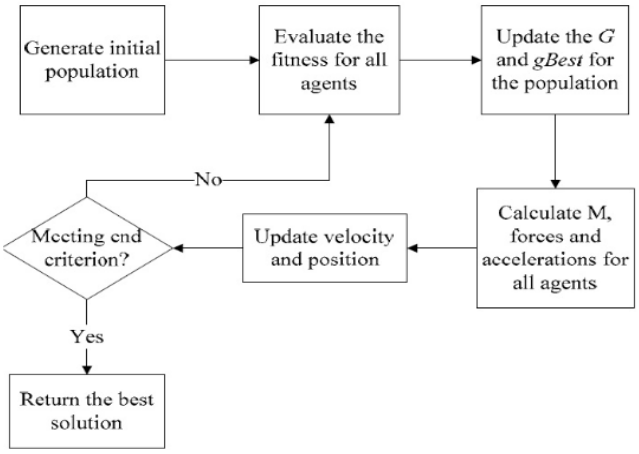

Fig. 3 The PSOGSA steps [30]:

V. RESULTS & DISCUSSION

The upper and lower bounds parameters for the typical FOPID and PID controller given in Table 1. The PSOGSA is used in order to tune and optimize the FOPID and PID coefficients: γ = [K_p, K_i, K_d, α, β]. The number of populations is selected as 10, $G_0 = 1, \gamma = 20$, $c_1 = 1.2, c_2 = 1.5$, r_1, r_2, ω are taken randon from [0,1], the maximum number of iterations is chosen as 100. The PSOGSA is used to find the appropriate values of the FOPID and PID controller's parameters to minimize the objective functions. In addition, the convergence rate for PSOGSA objective functions is shown in Figure 4. The objective function is defined according to the motion trajectory error of joints is given as follows [27]:

$$O = \sqrt{\int_0^\infty |e_1(t)|^2\, dt} + \sqrt{\int_0^\infty |e_2(t)|^2\, dt} \quad (10)$$

Where, $e_1(t) = q_1(t) - q_{d1}(t)$ and $e_2(t) = q_2(t) - q_{d2}(t)$.

Table 1. FOPID and PID upper and lower bounds

Control Strategy		**K_p**	**K_i**	**K_i**	**α**	**β**
FOPID	Min Max	0 1000	0 1000	0 1000	0.1 0.95	0.1 0.95
PID	Min Max	0 1000	0 1000	0 1000	0.1 0.95	0.1 0.95

The desired motion trajectory is given as follows [27]:

$$\theta_{d1}(t) = \sin(4.17t)$$
$$\theta_{d2}(t) = 1.2\sin(5.11t)$$

The initial values of the system are selected as follows:

$$q_{d1} = \pi,\ q_{d1} = -\pi,\ \dot{q_{d1}}(t) = 0 \ and \ \dot{q_{d2}}(t) = 0$$

Following the optimization of FOPID and PID controllers using PSOGSA, the resulting controller parameters are detailed in Table 2. Additionally, the RMSE indices in Table 3 indicate that the tracking performance of the arm robot exhibits slight enhancements when employing FOPID as opposed to

conventional PID controller across the desired trajectories. Notably, the table underscores that FOPID demonstrates significantly reduced trajectory errors and exhibits a smaller RMSE when compared to alternative PID. This observation underscores the considerable superiority of the FOPID structure in the context of arm robot trajectory tracking. Figure 5 shows the position tracking control of q_1 and q_2 under the PID and FOPID. It can be seen from Figure 5 that using the FOPID obtains a faster and more efficient performance to the reference trajectory than the PID approach. The 2-DOF robot manipulator under FOPID can reach the desired trajectory faster than the PID controller, while the PID is also shown an acceptable response having a good performance. Figure 6 presents the position tracking error of q_1 and q_2 under FOPID and PID. As seen from Figure 6, FOPID has the least error of trajectory tracking followed by PID. According to Figure 5 and 6, the maximum overshoot is reduced and settling time is converged to zero in a limited time for q_1 and q_2 under FOPID. The velocity of joints 1 and 2 are shown in Figure 7 under applied controllers. According to Figure 7 the fastest controller is FOPID which makes the 2-DOF robot manipulator settles immediately to the set point in comparison to the other PID. In addition, a random noise is applied to verify the robustness of the proposed FOPIOD control method. Figure 8 shows that the proposed control method suitably suppressed applied noise. The assessment of performance relies on the root mean square error (RMSE), which is computed using the following formula:

$$RMSE = \sqrt{\frac{1}{n}\sum_{i=1}^{n}(X(i) - X_r(i))^2} \qquad (11)$$

Where, $X(i)$ and $X_r(i)$ denote vectors representing the actual and reference values at the *i-th* data point, respectively and n indicates the total number of data points.

Table 2. The obtained FOPID and PID parameters.

Control Strategy	$\mathbf{K_p}$	$\mathbf{K_i}$	$\mathbf{K_i}$	**α**	**β**
FOPID	867.2349	535.7817	535.7817	0.13395	0.13395
PID	878.3631	878.3631	878.3631	-	-

Table 3. The root mean squared error (RMSE) for different control strategies.

Control Strategy	**RMSE for θ1**	**RMSE for θ2**
FOPID	0.084813	0.044337
PID	0.12346	0.053864

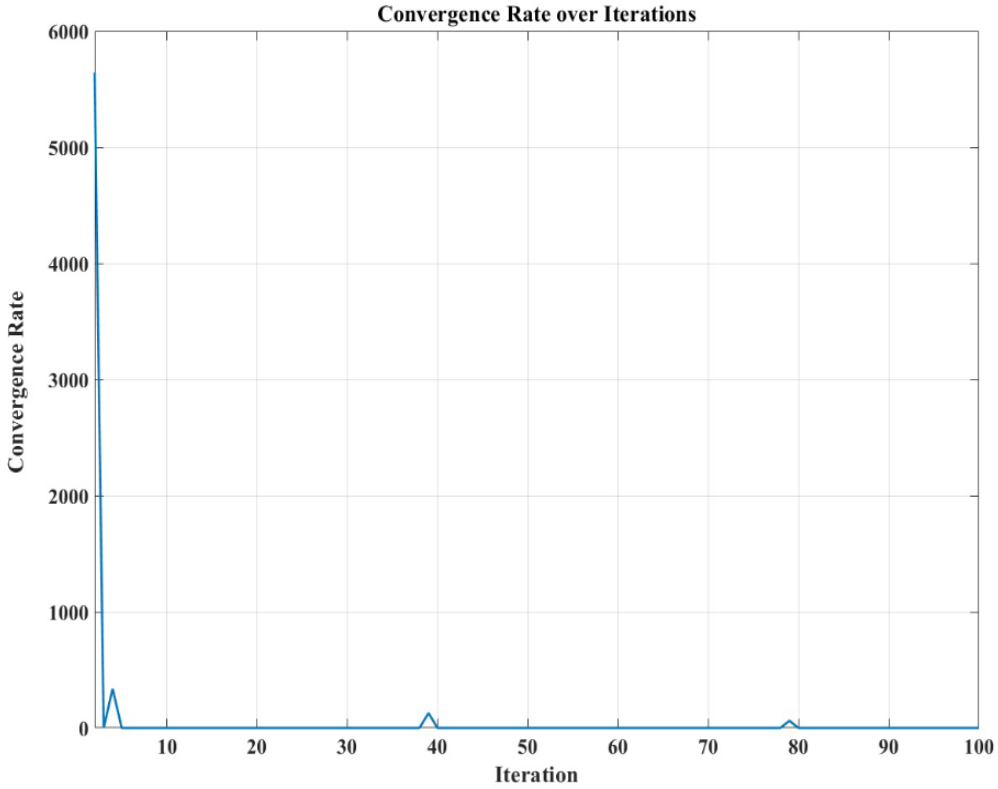

Fig. 4 The PSOGSA convergence rate under iterations

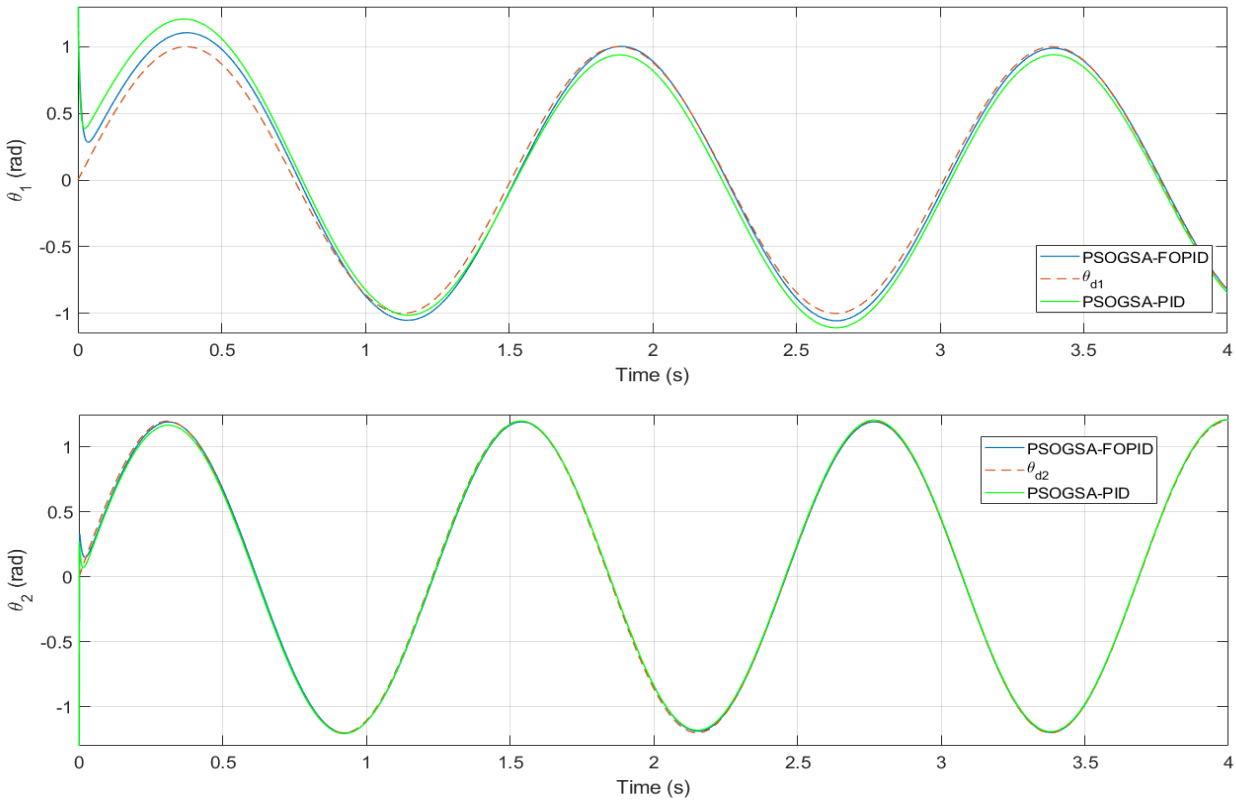

Fig. 5 Position tracking of joints under FOPID and PID controllers

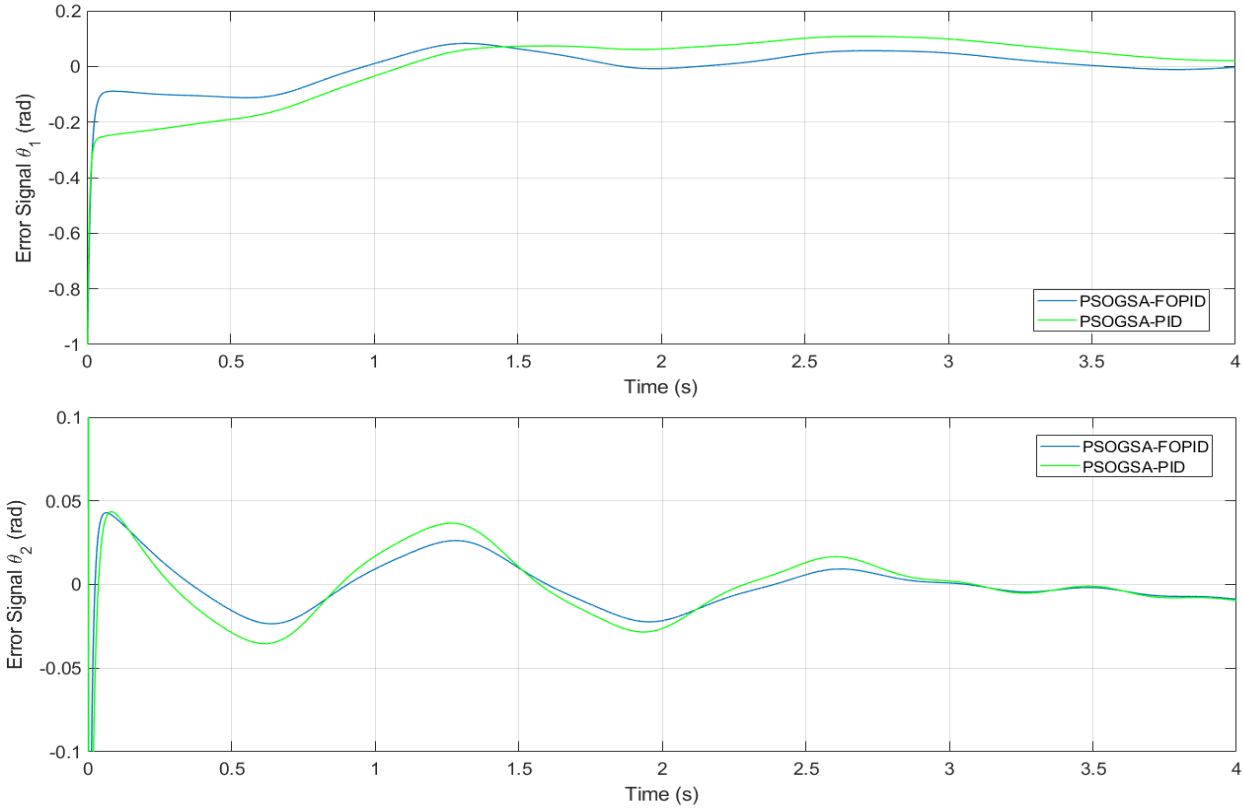

Fig. 6 Position tracking error of joints under FOPID and PID controllers

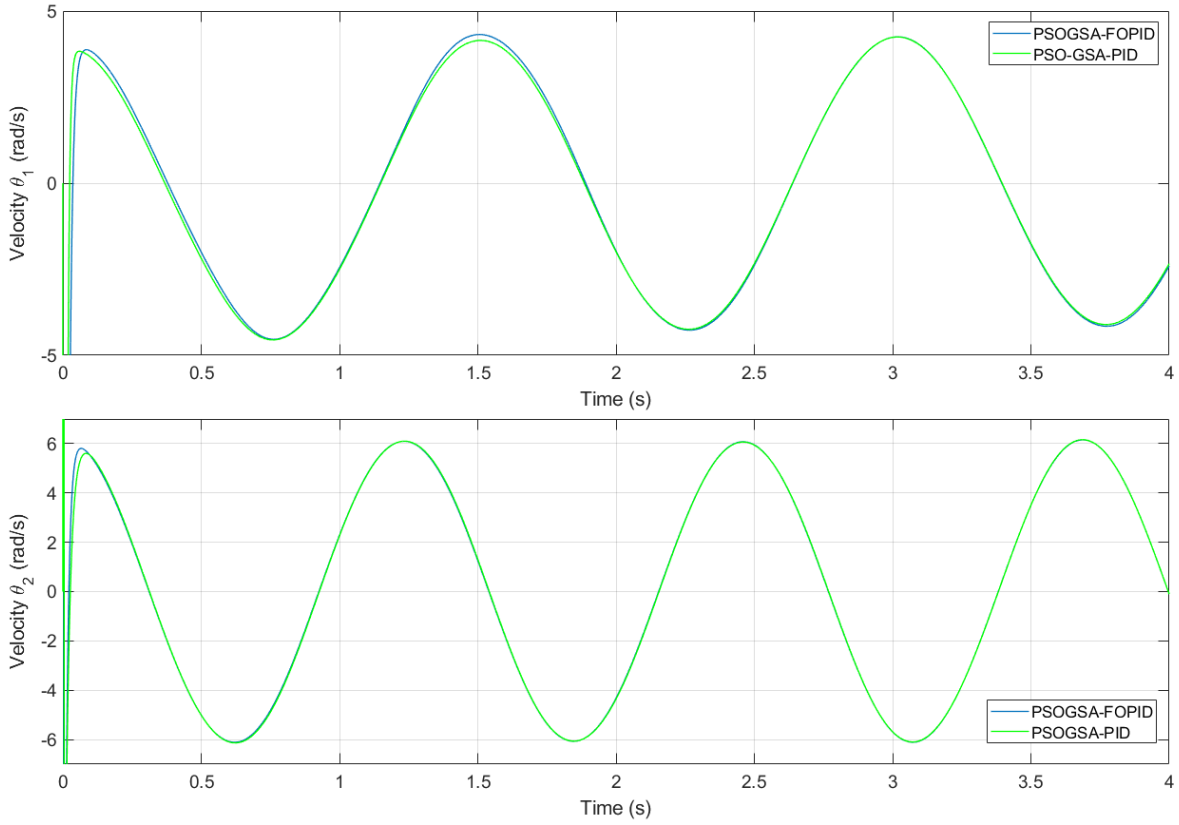

Fig.7.Velocity of joints under FOPID and PID controllers

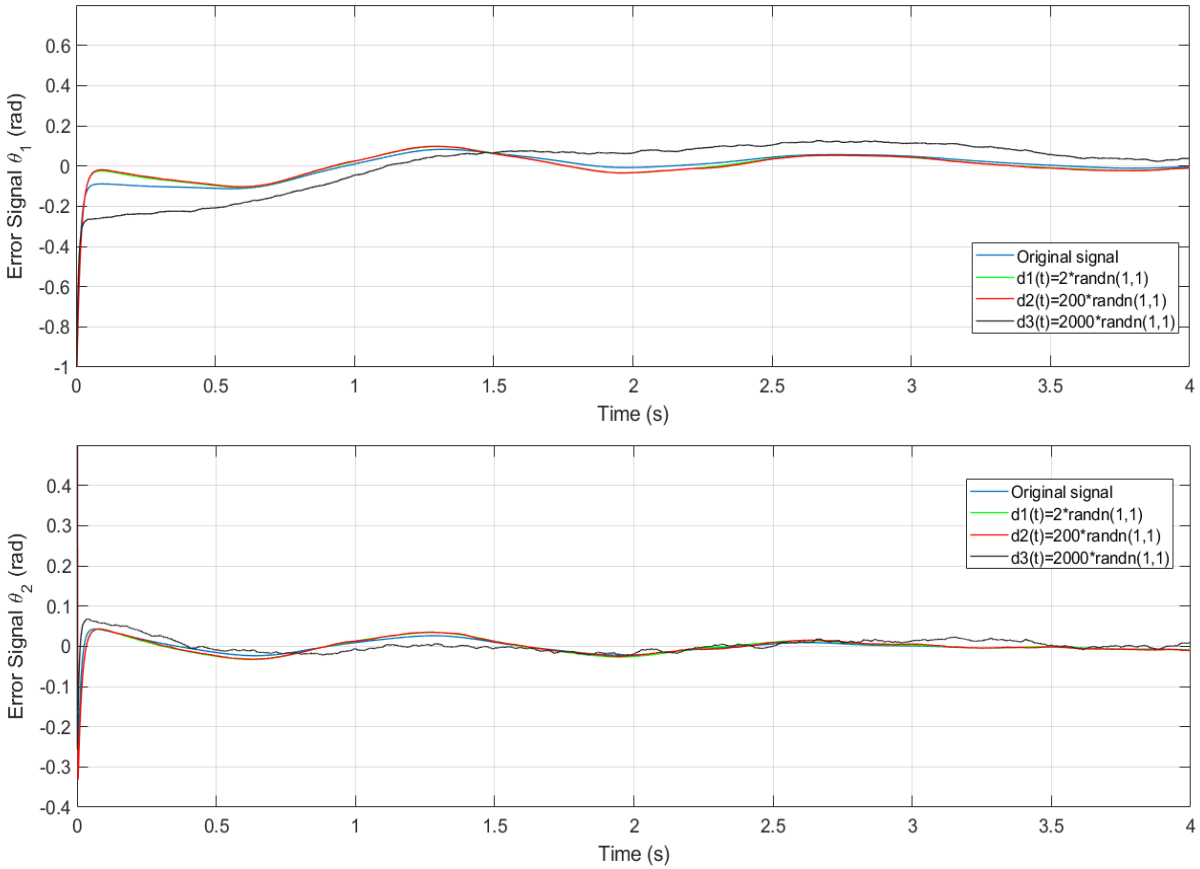

Fig. 8 Position tracking error of joints of the proposed controller under random noises application

VI. CONCLUSION

This paper addressed the trajectory tracking control for a 2-degree-of-freedom (2-DOF) robot manipulator through dynamic modeling, fractional-order PID (FOPID) and PID controllers. The dynamic model, expressed by a second-order differential equation, considered inertia, Coriolis and centrifugal effects and gravitational forces. Both FOPID and PID controllers were designed to regulate joint angles to follow desired trajectories. The PSOGSA algorithm was employed to tune and optimize the controller parameters.

Simulation results demonstrated the superior performance of the FOPID controller over the traditional PID controller. The FOPID controller, with optimized parameters obtained through PSOGSA, exhibited reduced trajectory errors and smaller root mean squared error (RMSE) values, indicating enhanced tracking precision compared to PID.

The proposed FOPID control, optimized through PSOGSA, showcased significant advancements in trajectory tracking and control efficiency for the 2-DOF robot manipulator. The results contribute to the field of robotics by emphasizing the effectiveness of advanced control strategies in improving the performance of robotic systems, particularly in trajectory tracking applications.

ACKNOWLEDGMENT

The authors extend their sincere appreciation to the Telecommunications Signals and Systems Laboratory (TSS), University Amar Telidji, and the Engineering School of Vitoria, University of the Basque Country UPV/EHU, Vitoria, Spain.

REFERENCES

[1] Jin L, Li S, Yu J, et al. Robot manipulator control using neural networks: A survey. Neurocomputing. 2018; 285:23–34.
[2] Silaa MY, Derbeli M, Barambones O, et al. Design and implementation of high order sliding mode control for pemfc power system. Energies. 2020;13(17):4317.
[3] Silaa MY, Barambones O, Bencherif A. A novel adaptive pid controller design for a pem fuel cell using stochastic gradientdescent with momentum enhanced by whale optimizer. Electronics. 2022;11(16):2610.
[4] Silaa MY, Barambones O, Cortajarena JA, et al. Pemfc current control using a novel compound controller enhanced by the black widow algorithm: A comprehensive simulation study. Sustainability. 2023;15(18):13823.
[5] Whig P, Bhatia B, Bhatia AB, et al. Renewable energy optimization system using fuzzy logic. In: Machine learning and metaheuristics: Methods and analysis. Springer; 2023. p. 177–198.
[6] Eker M, G ̈undogan B. Demagnetization fault detection of permanent magnet synchronous motor with convolutional neural network. Electrical Engineering. 2023;1–14.
[7] Jin M, Lee J, Chang PH, et al. Practical nonsingular terminal sliding-mode control of robot manipulators for high-accuracy tracking control. IEEE Transactions on Industrial Electronics. 2009;56(9):3593–3601.
[8] Bi M. Control of robot arm motion using trapezoid fuzzy two-degree-of-freedom pid algorithm. Symmetry. 2020;12(4):665.
[9] Jouila A, Nouri K. An adaptive robust nonsingular fast terminal sliding mode controller based on wavelet neural network for a 2-dof robotic arm. Journal of the Franklin Institute. 2020;357(18):13259–13282.
[10] Efe M ̈O. Fractional fuzzy adaptive sliding-mode control of a 2-dof direct-drive robot arm. IEEE Transactions on Systems, Man, and Cybernetics, Part B (Cybernetics). 2008; 38(6):1561–1570.
[11] Kumar A, Kumar V. Evolving an interval type-2 fuzzy pid controller for the redundant robotic manipulator. Expert Systems with Applications. 2017; 73:161–177.
[12] Ouyang P, Acob J, Pano V. Pd with sliding mode control for trajectory tracking of robotic system. Robotics and Computer-Integrated Manufacturing. 2014;30(2):189–200.
[13] Kallu KD, Jie W, Lee MC. Sensorless reaction force estimation of the end effector of a dual-arm robot manipulator using sliding mode control with a sliding perturbation observer. International Journal of Control, Automation and Systems. 2018;16(3):1367– 1378.
[14] Jung S. Improvement of tracking control of a sliding mode controller for robot manipulators by a neural network. International Journal of Control, Automation and Systems. 2018; 16:937–943.
[15] Mobayen S. Adaptive global terminal sliding mode control scheme with improved dynamic surface for uncertain nonlinear systems. International Journal of Control, Automation and Systems. 2018; 16:1692–1700.
[16] Liu Y. Sliding mode control for a class of uncertain discrete switched systems. International Journal of Control, Automation and Systems. 2018; 16:1716–1723.
[17] Mnasri C, Chorfi D, Gasmi M. Robust integral sliding mode control of uncertain networked control systems with multiple data packet losses. International Journal of Control, Automation and Systems. 2018; 16:2093–2102.
[18] Cao Z, Niu Y, Zhao H. Finite-time sliding mode control of markovian jump systems subject to actuator faults. International Journal of Control, Automation and Systems. 2018; 16:2282–2289.
[19] Zhao H, Niu Y. Guaranteed cost sliding mode control of switched systems with known sojourn probabilities. International Journal of Control, Automation and Systems. 2018; 16:2822–2831.
[20] Mirjalili S, Mirjalili SM, Lewis A. Grey wolf optimizer. Advances in engineering software. 2014; 69:46–61.
[21] Razmjooy N, Ramezani M, Namadchian A. A new lqr optimal control for a single-link flexible joint robot manipulator based on grey wolf optimizer. Majlesi Journal of Electrical Engineering. 2016;10(3):53.
[22] Sanjay R, Jayabarathi T, Raghunathan T, et al. Optimal allocation of distributed generation using hybrid grey wolf optimizer. Ieee Access. 2017; 5:14807–14818.
[23] Li L, Sun L, Kang W, et al. Fuzzy multilevel image thresholding based on modified discrete grey wolf optimizer and local information aggregation. Ieee Access. 2016; 4:6438–6450.
[24] Zhao L, Wang X. A deep feature optimization fusion method for extracting bearing degradation features. IEEE Access. 2018; 6:19640–19653.
[25] S ̧EN MA, KALYONCU M. Optimal tuning of pid controller using grey wolf optimizer algorithm for quadruped robot. Balkan Journal of Electrical and Computer Engineering. 2018;6(1):29–35.
[26] Suhail SA, Bazaz MA, Hussain S. Optimal tuned linear active disturbance rejection control applied to a 2-dof robotic arm manipulator. In: Proceedings of 6th International Conference on Recent Trends in Computing: ICRTC 2020; Springer; 2021. p. 665–675.
[27] Rahmani, M., Komijani, H., & Rahman, M. H. (2020). New sliding mode control of 2-DOF robot manipulator based on extended grey wolf optimizer. International Journal of Control, Automation and Systems, 18, 1572-1580.
[28] Divya Teja A, Kiranmayi R, Nagabhushanam K, et al. Simplified decoupler based fractional order pid controller for two variable fractional order process. In: International Conference on Artificial Intelligence for Smart Community: AISC 2020, 17–18 December, Universiti Teknologi Petronas, Malaysia; Springer; 2022. p. 35–47.
[29] Silaa MY, Barambones O, Derbeli M, et al. Fractional order pid design for a proton exchange membrane fuel cell system using an extended grey wolf optimizer. Processes. 2022;10(3):450.

[30] Mirjalili, S., & Hashim, S. Z. M. (2010, December). A new hybrid PSOGSA algorithm for function optimization. In 2010 international conference on computer and information application (pp. 374-377). IEEE.

APPENDIX A

The calculation of the parameters for the dynamics of a 2-DoF robot manipulator, as presented in equation (1), is as follows:

$$q = \begin{bmatrix} \theta_1 \\ \theta_2 \end{bmatrix}$$

$$B(q) = \begin{bmatrix} B_{11} & B_{12} \\ B_{21} & B_{22} \end{bmatrix}$$

Where,

$$B_{11} = (m_1 + m_2) \cdot l_1^2 + m_2 \cdot l_1^2 + 2 \cdot m_2 \cdot l_1 \cdot l_2 \cdot \cos(\theta_2)$$
$$B_{12} = m_2 \cdot l_2^2 + m_2 \cdot l_1 \cdot l_2 \cdot \cos(\theta_2)$$
$$B_{21} = m_2 \cdot l_2^2 + m_2 \cdot l_1 \cdot l_2 \cdot \cos(\theta_2)$$
$$B_{22} = m_2 \cdot l_2^2$$

$$C(q, \dot{q}) = \begin{bmatrix} -m_2 \cdot l_1 \cdot l_2 \cdot \sin(\theta_2) \cdot (2 \cdot \dot{\theta_1} \cdot \dot{\theta_2} + \dot{\theta_2} + \dot{\theta_2^2}) \\ -m_2 \cdot l_1 \cdot l_2 \cdot \sin(\theta_2) \cdot \dot{\theta_2} + \dot{\theta_2} \end{bmatrix}$$

$$G(q) = \begin{bmatrix} -(m_1 + m_2) \cdot g \cdot l_1 \cdot \sin(\theta_1) - m_2 \cdot g \cdot l_2 \sin(\theta_1 + \theta_2) \\ -m_2 \cdot g \cdot l_2 \cdot \sin(\theta_1 + \theta_2) \end{bmatrix}$$

$$\tau = \begin{bmatrix} \tau_1 \\ \tau_2 \end{bmatrix}$$

Where, $m_1 = m_2$=1, $l_1 = l_2$=1 and g=9.8